Journal of Information Systems Engineering and Management
2025, 10(4)
e-ISSN: 2468-4376
https://www.jisem-journal.com/

Research Article

Advanced Trajectory Control of a Hexacopter UAV: Comparative Analysis of Nonsingular Terminal Sliding Mode and PID Controllers

Said Khoudiri [1], Abdelkader Khoudiri [1], Mohamed Boudiaf [1], Mohamed Elbar [2]
[1] *Renewable Energy Systems Applications Laboratory (LASER), University of Djelfa, PO, Box 3117, 17000 Djelfa, Algeria*
[2]*Applied Automation and Industrial Diagnostics Laboratory (LAADI), Faculty of Science and Technology, Ziane Achour University, Djelfa 17000, Algeria.*

ARTICLE INFO

Received: 10 Nov 2024
Revised: 25 Dec 2024
Accepted: 22 Jan 2025

ABSTRACT

Introduction: This study presents a control strategy for trajectory tracking of Hexacopter UAVs using sliding mode control. The Hexacopter's nonlinear mathematical model is first derived using Newton-Euler's formulation. A nonsingular fast terminal sliding mode controller (NSTSMC) is then developed to enable precise tracking of the flight trajectory, while accommodating variations in orientation angle. To evaluate the controller's robustness, additional disturbances and chattering reduction techniques are introduced in the tests. The control system's performance, compared with a classical PID controller, is assessed using MATLAB-Simulink simulations. The results demonstrate that the Hexacopter, under the NSTSMC, effectively mitigates disturbances with minimal deviation from the planned trajectory, requiring less effort.

Keywords: Hexacopter, Newton-Euler formalism, Nonsingular terminal sliding mode control, PID controller

INTRODUCTION

Research and development in the field of UAVs have witnessed a significant surge lately, owing to their wide-ranging applications in fields such as military operations, sports, weather, traffic, and search and rescue, among others. Initially, the focus was limited to quadcopters; However, due to the lack of redundancy of the rotor components of the quadrotor, researchers have now expanded their horizon to more multirotors and the various benefits they offer over Quadcopters[1] [2] [3] [4]. For instance, Hexacopters exhibit better flight time, greater fault tolerance capacity due to the redundant actuators in the system [5] [6], higher stability, and higher load-carrying capability. But its benefits come at a cost: the Hexacopter has highly nonlinear dynamics, coupled and is underactuated. [7] [8] Under-actuated systems have a smaller number of control inputs compared to the system's degrees of freedom. They are difficult to control due to the nonlinear coupling between the actuators and the degrees of freedom. [2] Hence, it is necessary to choose an adequate control law with certain robustness. Many controls have been proposed [9] [10] [11] [12]. Even though most common flight controllers are linear flight controllers, these can only be performed when the Hexacopter is hovering around; they suffer from huge performance degradation whenever the Hexacopter is outside the nominal conditions or performs aggressive maneuvers [13]. In this work, a nonsingular terminal sliding mode control is designed and compared in our case with a PID controller. The paper is organized as follows: First, the dynamic mathematical model of the Hexacopter will be formulated using the Newton-Euler method. Then, the proposed control will be presented and discussed in terms of dynamic performance and stability to prove its quality, the conclusion is drawn in the last section.

DESCRIPTION AND MODELING OF THE HEXACOPTER

The mathematical representation of the Hexacopter must accurately depict its attitude based on the established geometric configuration. [14] This UAV is composed of a rigid body with a symmetrical structure with six propellers positioned orthogonally along the frame. When a drone moves in the air, various forces act on it. The resultant force

Journal of Information Systems Engineering and Management
2025, 10(4)
e-ISSN: 2468-4376
https://www.jisem-journal.com/

Research Article

will decide its movement. The major forces acting on the drone are thrust, lift (the force against gravity), drag, and weight. Figure 01 gives the schematic structure of the Hexacopter.

The configuration demonstrates three movements that encompass all possible attitude combinations: The Roll ϕ, which involves rotation around the X axis is achieved by adjusting the balance of rotors 1, 2, and 3 (or 6, 5, and 4) through speed changes. Lateral acceleration is attained by altering this angle; The pitch θ involves a rotation around the Y axis, and it is achieved by adjusting the balance of the speed of rotors 1 and 6 (or 3 and 4), changing this angle leads to longitudinal acceleration; Finally, the yaw ψ involves a rotation about the Z-axis and obtained by simultaneously adjusting the speed of motors 1, 3, and 5 or the motors 2, 4, and 6.

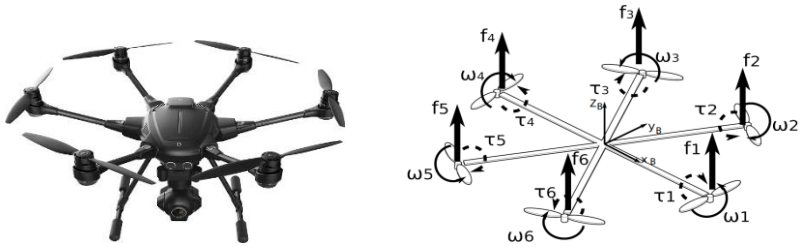

Figure 1. Schematic of the Hexacopter

To drive the state space dynamic model for the position and orientation of the Hexacopter, Newton-Euler formalism is applied [8] [14], taking the inertial frame quantities as state variables, the position and the orientation of the vehicle in the inertial frame are given by the vector: $X_p = [x, y, z, \phi, \theta, \psi]^T$. This vector is obtained initially from the body frame using the following transformations: R_{pB}^E for the position, and R_{oB}^E for the orientation.

$$R_{pB}^E = \begin{bmatrix} \cos\theta\cos\psi & \cos\psi\sin\theta\sin\phi - \sin\psi\cos\phi & \cos\psi\sin\theta\cos\phi + \sin\psi\sin\phi \\ \sin\psi\cos\theta & \sin\theta\sin\psi\sin\phi + \cos\psi\cos\theta & \cos\phi\sin\psi\sin\theta - \cos\psi\sin\phi \\ -\sin\theta & \sin\phi\cos\theta & \cos\theta\cos\phi \end{bmatrix} \quad (1)$$

$$R_{oB}^E = \begin{bmatrix} 1 & 0 & -sin\theta \\ 0 & cos\phi & sin\phi cos\theta \\ 0 & -sin\phi & cos\phi cos\theta \end{bmatrix} \quad (2)$$

The following equations give the model using the formalism [4]:

$$\begin{bmatrix} mI_{3\times3} & 0_{3\times3} \\ 0_{3\times3} & J \end{bmatrix} \begin{bmatrix} \dot{V} \\ \dot{\omega} \end{bmatrix} + \begin{bmatrix} \omega \times \omega V \\ \omega \times J\omega \end{bmatrix} = \begin{bmatrix} \sum F \\ \sum T \end{bmatrix} \quad (3)$$

Where: F is the net force acting on the center of mass ; T is the resultant torque acting on the center of mass
m is the mass of the body ; V is the velocity of the center of mass, ω is the angular velocity of the body,
J is the Moment of inertia about the center of mass.

For a symmetric UAV: $$J = \begin{bmatrix} J_{xx} & 0 & 0 \\ 0 & J_{yy} & 0 \\ 0 & 0 & J_{zz} \end{bmatrix} \quad (4)$$

The dynamic model of the Hexacopter is made by including the analysis of the following forces that affect the Hexacopter movements and their vectors in the body frame: gravity, thrust, rotor drag, and air friction.

1-The Gravity force: $$F_g = [0 \quad 0 \quad mg]^T \quad (5)$$

Where: m is the mass of the Hexacopter, and g is the gravitational acceleration.

2-The Thrust force along the z-axis: $$F_T = R_{pB}^E \begin{bmatrix} 0 & 0 & k_t . \sum_1^6 \Omega_i^2 \end{bmatrix}^T \quad (6)$$

Where: k_t is the thrust factor, and Ω_i is the angular velocity of propeller i

3-The rotor drag : $$F_r = I_{3\times3}\begin{bmatrix} k_{rx} & k_{ry} & k_{rz} \end{bmatrix}^T . X \quad (7)$$

Where: diag $\begin{bmatrix} k_{rx} & k_{ry} & k_{rz} \end{bmatrix}$ is the vector of drag coefficient forces ; k_r is the drag factor

Journal of Information Systems Engineering and Management
2025, 10(4)
e-ISSN: 2468-4376
https://www.jisem-journal.com/

Research Article

4-The Air resistance for each propeller $F_{ai} = k_r \Omega_i^2$ (8)

In addition, the main existent torques effects are:

a. Actuator action

- Roll torque: $T_X = k_t l \frac{\sqrt{3}}{2}\left(-\Omega_1^2 + \Omega_5^2 + \frac{1}{2}(-\Omega_1^2 - \Omega_3^2 + \Omega_4^2 + \Omega_6^2)\right)$ (9)

With: l is the arm length

- Pitch torque: $T_y = k_t l \frac{\sqrt{3}}{2}(-\Omega_1^2 + \Omega_3^2 + \Omega_4^2 - \Omega_6^2)$ (10)

- Yaw torque: $T_z = k_r(-\Omega_1^2 + \Omega_2^2 - \Omega_3^2 + \Omega_4^2 - \Omega_5^2 + \Omega_6^2)$ (11)

The three torques angles are regrouped as : $T_T = [T_X\ T_y\ T_z]^T$

- Reaction torque: $T_r = [0,0,J\dot{\Omega}_r]^T$ (12)

With: $\Omega_r = \sum_1^6 (-1)^2 \Omega_i$

b. Torque aerodynamic resistance: $T_a = k_a \omega^2 = [k_{ax}\dot{\phi}^2\ \ k_{ay}\dot{\theta}^2\ \ k_{az}\dot{\psi}^2]^T$ (13)

With: k_a is the aerodynamic force constant.

c. Gyroscopic effect: $T_G = \begin{bmatrix} \dot{\theta} J\Omega_r \\ \dot{\phi} J\Omega_r \\ 0 \end{bmatrix}$ (14)

Translational and rotational dynamics

Applying the forces and torques expressions, in the model (3) allows to obtain the equations that govern the translational and the rotational motion for the Hexacopter with respect to the body frame:

$$F_T - F_g - F_r = m\dot{X_p} \quad (15)$$

$$T_T - T_r - T_a - \omega \times J\omega = J\dot{\omega} \quad (16)$$

Thus: $\ddot{x} = 1/m(cos\phi sin\theta cos\psi - sin\phi sin\psi)(\sum_{i=1}^6 F_i) - k_{rx}\dot{x}/m$ (17)

$$\ddot{y} = 1/m(cos\phi sin\theta sin\psi - sin\phi cos\psi)(\sum_{i=1}^6 F_i) - k_{ry}\dot{y}/m \quad (18)$$

$$\ddot{z} = 1/m(sin\phi cos\theta)(\sum_{i=1}^6 F_i) - k_{rz}\dot{z}/m - g \quad (19)$$

And $J_{xx}\ddot{\phi} = \dot{\theta}\dot{\psi}(J_{yy} - J_{zz}) - k_{ax}\dot{\phi}^2 - J\Omega_r\dot{\theta} + k_t l\left(-\Omega_2^2 + \Omega_5^2 + \frac{1}{2}(-\Omega_1^2 - \Omega_3^2 + \Omega_4^2 + \Omega_6^2)\right)$ (20)

$$J_{yy}\ddot{\theta} = \dot{\phi}\dot{\psi}(J_{zz} - J_{xx}) - k_{ay}\dot{\theta}^2 + J\Omega_r\dot{\phi} + k_t l\frac{\sqrt{3}}{2}(-\Omega_1^2 + \Omega_3^2 + \Omega_4^2 - \Omega_6^2) \quad (21)$$

$$J_{zz}\ddot{\psi} = \dot{\phi}\dot{\theta}(J_{xx} - J_{yy}) - k_{az}\dot{\psi}^2 + k_r(-\Omega_1^2 + \Omega_2^2 - \Omega_3^2 + \Omega_4^2 - \Omega_5^2 + \Omega_6^2) \quad (22)$$

The Hexacopter rotational speeds are related to the aerodynamic thrust force and torques. The system has four defined control inputs given by:

$$U = [U_1 U_2 U_3 U_4]^T \quad (23)$$

U_1 is the control input for the altitude which causes the upward thrust force. U_2 is the difference in rotors thrust 1,2,3 and 4,5,6 which makes the roll movement. U_3 is a control input that represents the difference of rotors thrust 1,6 and 3,4 and it is responsible for the pitch rotation. Finally, U_4 is the difference in rotors torque between the three clockwise rotating rotors and the three counterclockwise rotating rotors that generates the yaw rotation; then, the rotor velocities are calculated as:

$$\begin{bmatrix} \Omega_1^2 \\ \Omega_2^2 \\ \Omega_3^2 \\ \Omega_4^2 \\ \Omega_5^2 \\ \Omega_6^2 \end{bmatrix}^T = \begin{bmatrix} U_1 \\ U_2 \\ U_3 \\ U_4 \end{bmatrix}^T \begin{bmatrix} k_t & k_t & k_t & k_t & k_t & k_t \\ \frac{-k_t l}{2} & -k_t l & \frac{-k_t l}{2} & \frac{k_t l}{2} & k_t l & \frac{k_t l}{2} \\ \frac{-\sqrt{3}k_t l}{2} & 0 & \frac{\sqrt{3}k_t l}{2} & \frac{\sqrt{3}k_t l}{2} & 0 & \frac{-\sqrt{3}k_t l}{2} \\ -k_r & k_r & -k_r & k_r & -k_r & k_r \end{bmatrix}^{-1} \quad (24)$$

Journal of Information Systems Engineering and Management
2025, 10(4)
e-ISSN: 2468-4376
https://www.jisem-journal.com/

Research Article

Using relation (17) to (22), the position and orientation dynamical state-space model of a Hexacopter can be rewritten in the disturbed form; assuming that:
The Euler angles are bounded as : ϕ and θ]- π /2 , π /2[; ψ]-π ,π [, f_i and g_i are smooth known , g_i non singular, and the un-modeled dynamics and external perturbations are included in the bounded functions Δ_i(t) .

Hence:
$$\dot{X}_{11} = X_{12} \tag{25}$$
$$\dot{X}_{12} = f_1(X,t) + g_1(X,t)U_a + \Delta_1(t)$$
$$\dot{X}_{21} = X_{22} \tag{26}$$
$$\dot{X}_{22} = f_2(X,t) + g_2(X,t)U_b + \Delta_2(t)$$

With: $X_{11} = [x\ y\ z]^T = [x_1 x_3 x_5]^T,\ \dot{X_{11}} = X_{21} = [\dot{x}\ \dot{y}\ \dot{z}\ ]^T = [x_2 x_4\ x_6]^T$

$$X_{12} = [\phi\ \theta\ \psi]^T = [x_7 x_9 x_{11}]^T, \quad \dot{X_{12}} = X_{22} = \left[\dot{\phi}\ \dot{\theta}\ \dot{\psi}\right]^T = [x_8 x_{10} x_{12}]^T$$

$$f_1(X,t) = \begin{bmatrix} -\frac{k_{rx}}{m}x_2 \\ -\frac{k_{ry}}{m}x_4 \\ -\frac{k_{rz}}{m}x_6 - g \end{bmatrix} ; \quad g_1(X,t) = \begin{bmatrix} \frac{1}{m}[cosx_7 sinx_9 cosx_{11} + sinx_7 sinx_{11}] \\ \frac{1}{m}[cosx_7 sinx_9 sinx_{11} + sinx_7 cosx_{11}] \\ \frac{1}{m}[cosx_9 cosx_{11}] \end{bmatrix}$$

$$f_2(X,t) = \begin{bmatrix} \left(\frac{Jyy-Jzz}{Jxx}\right)x_{10}x_{12} - \left(\frac{J\Omega_r}{Jxx}\right)x_{10} - k_{ax}{x_8}^2 \\ \left(\frac{Jyy-Jzz}{Jxx}\right)x_{10}x_{12} - \left(\frac{J\Omega_r}{Jxx}\right)x_{10} - k_{ax}{x_8}^2 \\ \left(\frac{Jxx-Jyy}{Jzz}\right)x_8 x_{10} - k_{az}{x_{12}}^2 \end{bmatrix} \quad ; \quad g_2(X,t) = \begin{bmatrix} \frac{l}{Jxx} \\ \frac{l}{Jyy} \\ \frac{l}{Jzz} \end{bmatrix}$$

Design of the controller

Since the Hexacopter is a nonlinear under-actuated system, it depends on both the translational and the rotational state variables. Six control dynamics are needed to track the desired trajectories and to regulate roll and pitch angles at the same time. The Sliding Mode Control is an appropriate technique to provide stabilization and tracking of the desired trajectory. The main advantage of Sliding Mode Control is that it has some robustness against model inaccuracies, parameter uncertainties, and disturbances [15] [16], although it suffers from the chattering phenomenon. This last will be reduced in our case , by replacing the signum function with the saturation function.
The control scheme has two cascaded loops:

The outer loop is the *X Y Z* motions control, its control low is obtained from the subsystem in eq. (25), its output U_a *(t)* contain the desired Altitude U_1 control as well as U_x and U_y to control translations in the *X* and *Y* axis, then, the desired roll ϕ_d and pitch θ_d dynamics are generated from using a corrector block, this bloc is an analytical inversion and it is given by:

$$\begin{bmatrix} \phi_d \\ \theta_d \end{bmatrix} = \begin{bmatrix} sin^{-1}\left(\frac{-cos\psi U_y + sin\psi U_x}{U_1}\right) \\ sin^{-1}\left(\frac{sin\psi U_y + cos\psi U_x}{U_1 cos\phi}\right) \end{bmatrix} \tag{27}$$

The inner loop is the orientation angles control, its output U_b *(t)* contain three control laws U_2 ,U_3,U_4, to control the dynamics of the three rotations angles. Finally, the calculation of the speed of the Rotor is achieved through the inversion of eq (27). The proposed control diagram is given by:

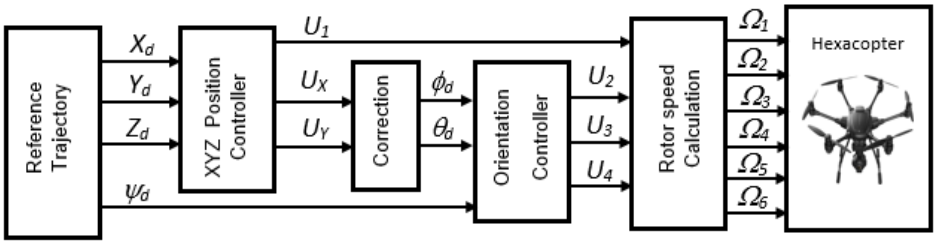

Figure 2. NSTSMC Block diagram of the Hexacopter

XYZ motions controller

Journal of Information Systems Engineering and Management
2025, 10(4)
e-ISSN: 2468-4376
https://www.jisem-journal.com/

Research Article

To control the *X* and *Y* motions in the presence of external disturbances *Δ1 (t)*, the fellowing subsystem is given:

$$\dot{X}_{11} = X_{12}$$
$$\dot{X}_{12} = f_1(X,t) + g_1(X,t)U_a + \Delta_1(t)$$

With : *f1 (X,t)* and *g1 (X,t)* are given in eq. (25) and eq. (26)
Note that here : $U_a = [U_x, U_y, U_1]^T$
Choosing the first Non-singular fast terminal sliding mode manifold for the *XYZ* movements:

$$S_1 = \dot{e_1} + \lambda_{11} {e_1}^{\alpha_1/\beta_1} + \lambda_{12}|e_1|^{\gamma_1} sign\,(e_1) \quad (28)$$

Where : $e_1 = X_{11_d} - X_{11}$ and λ11 , *λ12* are positives tuning parameters vectors for the three translations, and *α1* and *β1* are positive odd integers, which satisfy the following condition to avoid the singularity in *U1 (t)* :

$$1 < \alpha_1/\beta_1 < 2 \qquad \text{and} \quad \gamma_1 > 1 \quad (29)$$

The time derivative becomes :

$$\dot{S_1} = \ddot{e_1} + \frac{\lambda_{11}\alpha_1}{\beta_1} {e_1}^{\frac{\alpha_1}{\beta_1}-1}\dot{e_1} + \lambda_{12}|e_1|^{\gamma_1-1}\dot{e_1}$$
$$= (\ddot{X_{11_d}} - \ddot{X_{11}}) + (\frac{\lambda_{11}\alpha_1}{\beta_1} {e_1}^{\frac{\alpha_1}{\beta_1}-1}\dot{e_1} + \lambda_{12}|e_1|^{\gamma_1-1}\dot{e_1})(\dot{X_{11_d}} - \dot{X_{11}}) \quad (30)$$

Substituting the time derivate $\ddot{X_{11}}$:

$$\dot{S_1} = \ddot{X_{11_d}} - f_1(X,t) - g_1(X,t)U_a + \frac{\lambda_{11}\alpha_1}{\beta_1} {e_1}^{\frac{\alpha_1}{\beta_1}-1}\dot{e_1} + \lambda_{12}|e_1|^{\gamma_1-1}\dot{e_1} - \Delta_1(t)$$

Solving $\dot{S_1} = 0$, then, the chosen feedback controller is obtained:

$$U_a(t) = g_1(X,t)^{-1}\left(\ddot{X_{11_d}} - f_1(X,t) + \frac{\lambda_{11}\alpha_1}{\beta_1} {e_1}^{\frac{\alpha_1}{\beta_1}-1}\dot{e_1} + \lambda_{12}|e_1|^{\gamma_1-1}\dot{e_1} + u_{1dyn}\right) \quad (31)$$

Where : U_{adyn} is given by the following low:

$$u_{adyn} = -k_{11}|S_1|^{\frac{1}{2}} sign(S_1) - k_{12}\,S_1 \quad (32)$$

With : *k11* , *k12* are positives real numbers.

Through the choice of the main parameters *λ11, λ12* vectors and the gain rates *k11*, k*12* vectors, the tracking error converges to zero in finite time; Robustness to bounded perturbations/uncertainties properties of standard sliding mode control is maintained, also, through the choice of γ*1*, the system will have a fast convergence speed when it is far from the equilibrium state.

Stability analysis of the X and Y motions controller

To verify the stability of the first controller, Lyapunov's direct method is used. Let's first consider that the perturbation *Δ1 (t)* is bounded:

$$|\Delta_1(t)| \le b_1 \quad (33)$$

Where : *b1* denotes a bounded positive constant.
The Lyapunov candidate function *V1 (X,t)* is :

$$V_1(X,t) = \frac{1}{2}{S_1}^2(t) \quad (34)$$

To achieve stability, the derivative of Lyapunov's candidate function must be negative, thus:

$$V_1(\dot{X},t) = S_1\dot{S_1} < 0,\ S_1 \neq 0 \quad (35)$$
$$V_1(\dot{X},t) = S_1[\ddot{X_{11_d}} - f_1(X,t) - g_1(X,t)U_a(t) + \frac{\lambda_{11}\alpha_1}{\beta_1} {e_1}^{\frac{\alpha_1}{\beta_1}-1}\dot{e_1} + \lambda_{12}|e_1|^{\gamma_1-1}\dot{e_1} - \Delta_1(t)]$$

Obtained replacing the feedback control *U1 (t)* in closed loop form in the sliding surface dynamics $\dot{S_1}$, one obtains:

$$V_1(\dot{X},t) = S_1\left[k_{11}|S_1|^{\frac{1}{2}} sign(S_1) + k_{12}\,S_1 - \Delta_1(t)\right] = -S_1\left[u_{adyn} + \Delta_1(t)\right]$$

Therefore, the derivative of The Lyapunov function will be:

$$V_1(\dot{X},t) \le -k_{11}|S_1||S_1|^{\frac{1}{2}} - k_{12}{S_1}^2 + b_1|S_1| \le 0 \quad (36)$$

This leads to:

$$k_{11}|S_1|^{1/2} + k_{12}\,|S_1| \ge b_1 \quad (37)$$

Journal of Information Systems Engineering and Management
2025, 10(4)
e-ISSN: 2468-4376
https://www.jisem-journal.com/

Research Article

e.g., , the gain *k11* will be constrained as:

$$k_{11} \geq \frac{1}{|S_1|^{1/2}}(b_1 - k_{12}\,|S_1|) \tag{38}$$

Hence, to ensure stability, one needs the closed loop feedback control *Ua (t)* given by eq (31) and eq (32), to be greater than the magnitude of the external bounded disturbance *Δ1 (t)*. Finally, to reduce the chattering. the signum function is replaced, by the saturation function:

$$sat(S_1) = \begin{cases} S_1 \text{ if } -1 \leq S_1 \leq 1 \\ sign(S_1) \text{ else} \end{cases} \tag{39}$$

Orientation angles controller

In the same way, the design of the Non-singular terminal controller that forces the sliding mode, for the orientation angles, to zero, is done considering the presence of $|\Delta_2(t)| \leq b_2$

$$\dot{X}_{21} = X_{22}$$
$$\dot{X}_{22} = f_2(X,t) + g_2(X,t)U_b + \Delta_2(t)$$

Note that here : $U_b = [U_2, U_3, U_4]^T$

The second sliding manifold has the same form of S*1*:

$$S_2 = \dot{e_2} + \lambda_{21} {e_1}^{\alpha_2/\beta_2} + \lambda_{22}|e_2|^{\gamma_2} sign\,(e_2) \tag{40}$$

Where : $e_2 = X_{21_d} - X_{21}$and the tuning parameters vectors $\lambda 21, \lambda 22$ for the three angles control are chosen to take the same conditions as *S1* . The time derivative of the sliding manifold is :

$$\dot{S_2} = \ddot{X_{21_d}} - \ddot{X_{21}} + \left(\frac{\lambda_{21}\alpha_2}{\beta_2} {e_2}^{\frac{\alpha_2}{\beta_2}-1}\dot{e_2} + \lambda_{22}|e_2|^{\gamma_2-1}\dot{e_2}\right)\left(\dot{X_{21_d}} - \dot{X_{21}}\right) \tag{41}$$

Replacing $\ddot{X_{21}}$ from the the hexacopter subsystem model, then Solving $\dot{S_2} = 0$, the following controller is obtained:

$$U_b(t) = g_2(X,t)^{-1}\left(\ddot{X_{21_d}} - f_2(X,t) + \frac{\lambda_{21}\alpha_2}{\beta_2} {e_2}^{\frac{\alpha_2}{\beta_2}-1}\dot{e_2} + \lambda_{22}|e_2|^{\gamma_2-1}\dot{e_2} + u_{bdyn}\right) \tag{42}$$

With : U_{bdyn} is given by the following low:

$$u_{bdyn} = -k_{21}|S_2|^{1/2} sign(S_2) - k_{22}\,S_2 \tag{43}$$

Where : *k11* , *k12* vectors are positives real.

Again, the signum function is replaced by the saturation function *sat (S2)* to reduce the chattering phenomenon.

The parameters vectors λ*21, λ22 k21*, k*22* are used to ensure the tracking error converges to zero in finite time; also, through γ_2, the system will have a fast dynamic response when it is far from the equilibrium point. The robustness properties to bounded perturbations/uncertainties of the standard sliding mode control are maintained.

Stability analysis of the Altitude and orientation angles controller

The Lyapunov candidate function *V2 (X,t)* is :

$$V_2(X,t) = \frac{1}{2}{S_2}^2(t)$$

To achieve stability, the derivative of Lyapunov's candidate function must satisfy:

$$V_2(\dot{X},t) = S_2\dot{S_2} < 0,\ S_2 \neq 0 \tag{44}$$

In addition, by replacing the control *U(t)* by its expression in closed loop form in the derivative of sliding surface:

$$\dot{S_2} = u_{2dyn} + \Delta_2(t) \tag{45}$$

Therefore, the derivative of The Lyapunov function will be:

$$V_2(\dot{X},t) = S_2\left[k_{21}|S_2|^{\frac{1}{2}}\,\text{sign}(S_2) + k_{22}\,S_2 - \Delta_2(t)\right] = -S_2\left[u_{bdyn} + \Delta_2(t)\right]$$

Thus: $$V_2(\dot{X},t) \leq -k_{21}(t)|S_2||S_2|^{1/2} - k_{22}{S_2}^2 + b_2|S_2| \leq 0 \tag{46}$$

And, the gains will be constrained as:

$$k_{21}|S_2|^{1/2} + k_{22}\,|S_2| \geq b_2 \tag{47}$$

Journal of Information Systems Engineering and Management
2025, 10(4)
e-ISSN: 2468-4376
https://www.jisem-journal.com/

Research Article

Therefore, one needs the closed loop feedback control $Ub\ (t)$ to be greater than the magnitude of the external disturbance $\Delta_2\ (t)$.

SIMULATION OF THE HEXACOPTER UNDER THE NSTSMC COMPARED TO THE PID CONTROL

In this section the Hexacopter nonlinear model under the proposed control system is verified by simulation in MATLAB/Simulink, and compared to the results obtained by simulation using a classical PID control. The PID control bloc consists of 6 PID controller's blocs one for each state space variable $[x, y, z, \phi, \theta, \psi]$

The tuning of the three parameters of each k_{pi}, k_{ii}, k_{di} with $i \in [x,y,z,\phi,\theta,\psi]$ is done initially using Cohen-Coon Method followed by extensive trial-error, The same procedure is done for the NSTSMC controller considering the conditions on the parameters. The parameters used to perform the simulation are:

$$\alpha 1 = 0.6,\ \beta 1 = 0.4\ ,\ \gamma 1 = 3\ ,\ \lambda 12 = 0.1\ ,\ k11 = 1.5\ ,\ k22 = 0.01$$

For the PID controllers: $k_{pi}=4,\ k_{ii}=7.5,\ k_{di}=1.2,$ with $i \in [x,y,z]$

$k_{pi}=3,\ k_{ii}=1.5,\ k_{di}=2.5,$ with $i \in [\phi,\theta,\psi]$

The considered Hexacopter parameters are given in the following table:

Table 1. Parameters of the Hexacopter

Parameter	symbol	Value	Unit
Mass of the body	m	2.1	kg
Length of the arm	l	0.23	m
Acceleration due to gravity	g	9.81	ms
Moment of Inertia-X axis	J_{xx}	$3.8 \cdot 10^{-3}$	Kgm^2
Moment of Inertia-Y axis	J_{yy}	3.8·10-3	Kgm^2
Moment of Inertia-Z axis	J_{zz}	$7.1 \cdot 10^{-3}$	Kgm^2
Rotor inertia	J_r	$0.8 \cdot 10^{-3}$	Kgm^2
Trust factor	k_t	$4.58 \cdot 10^{-3}$	Ns^2
Drag factor	k_r	$1.037 \cdot 10^{-3}$	Nms

A trajectory was designed to test the NSTSMC controller; In the test trajectory, the Hexacopter tracks the trajectory from the origin (0,0,0); the simulated infinity trajectory is created at the same time with $t \leq 30s$,,he equations of trajectory are as follows:

$$\begin{aligned} X_d(t) &= 2 - 2\cos\left(\frac{\pi}{15}t\right) \\ Y_d(t) &= 2\sin\left(\frac{2\pi}{15}t\right) \\ Z_d(t) &= 4 - \cos\left(\frac{\pi}{15}t\right) \end{aligned} \tag{48}$$

Fellow the yaw angle $\psi_d(t)$ in (deg) is set as fellow

$$\psi_d(t) = \begin{cases} 0 \text{ if } 0 \leq t < 20 \\ 30 \text{ else} \end{cases} \tag{49}$$

In addition, to test the system response robustness against bounded disturbances $\Delta 1\ (t)$, perturbation is added from $t=15\ s$ to $t=30\ s$ in X,Y, and Z. The simulation results are given in below:

Journal of Information Systems Engineering and Management
2025, 10(4)
e-ISSN: 2468-4376
https://www.jisem-journal.com/

Research Article

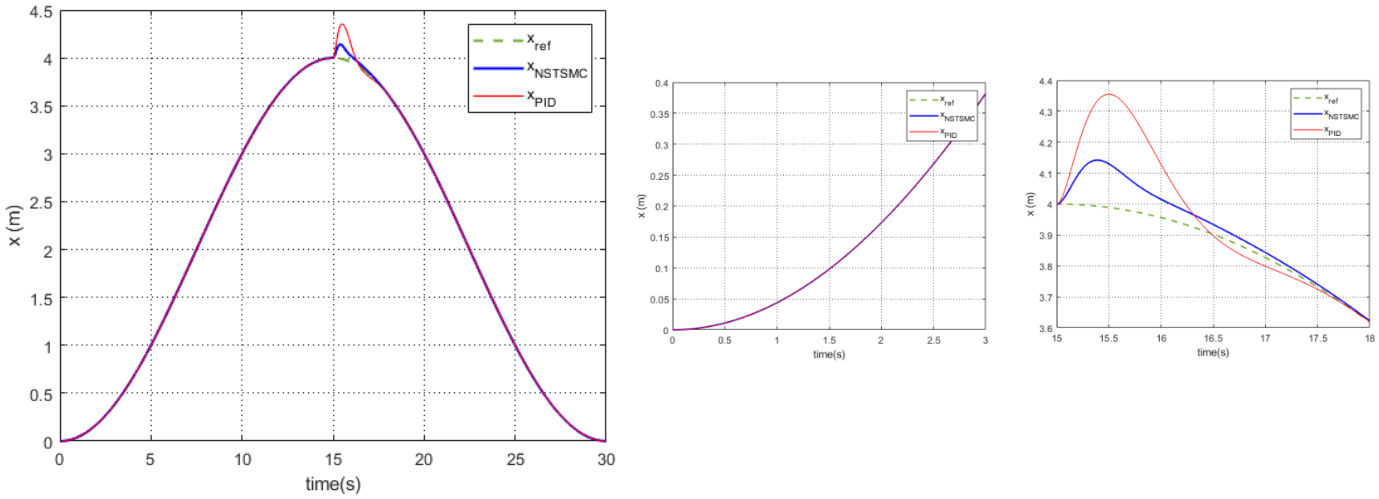

Figure 3. *X* position of the Hexacopter (with zoom)

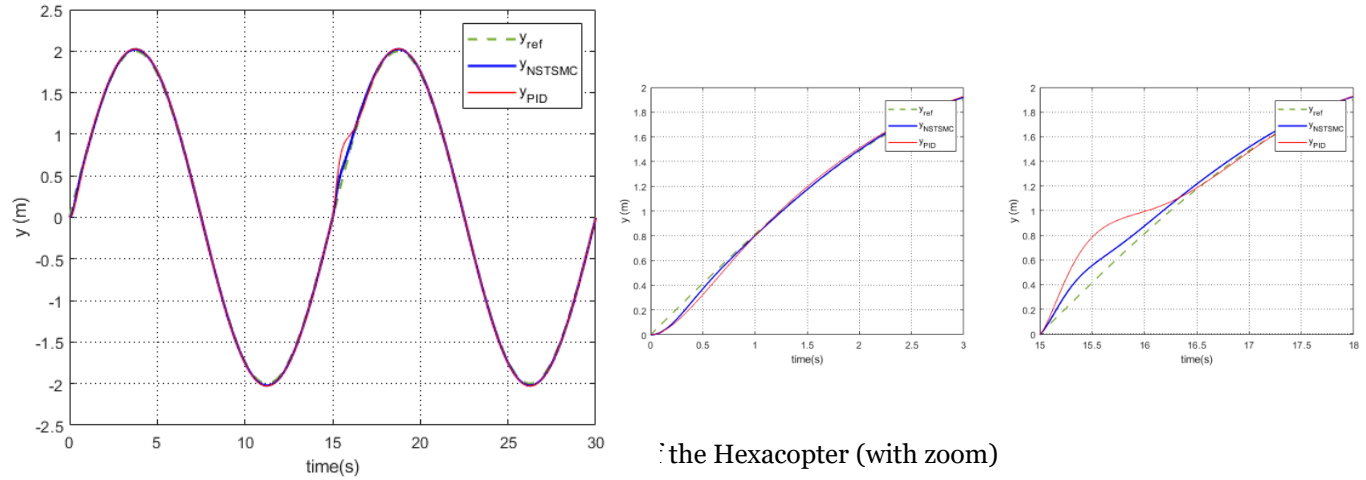

the Hexacopter (with zoom)

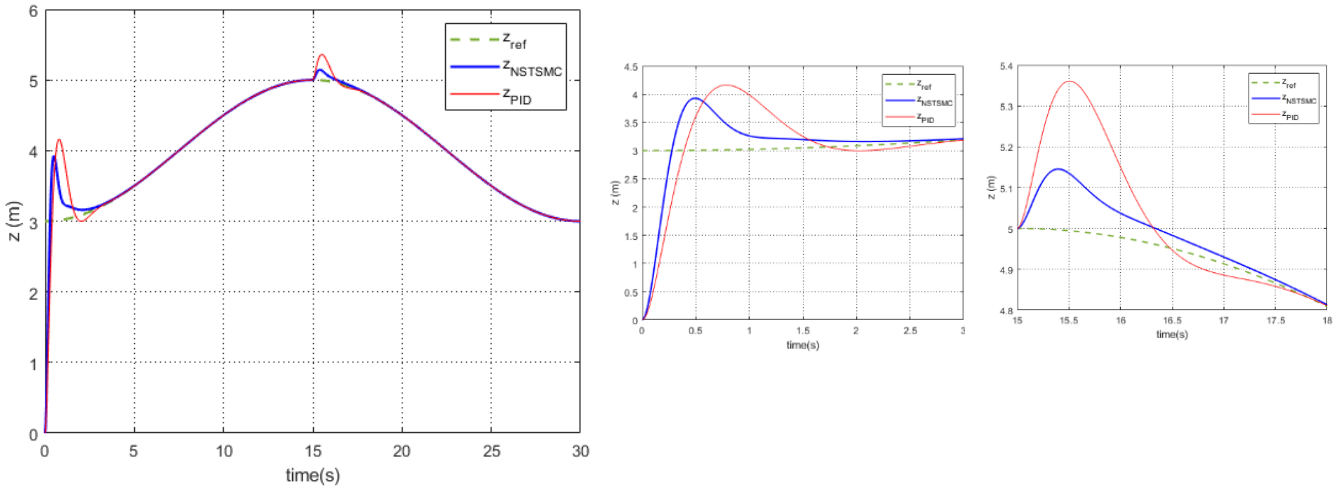

Figure 5. *Z* position of the Hexacopter (with zoom)

Journal of Information Systems Engineering and Management
2025, 10(4)
e-ISSN: 2468-4376
https://www.jisem-journal.com/

Research Article

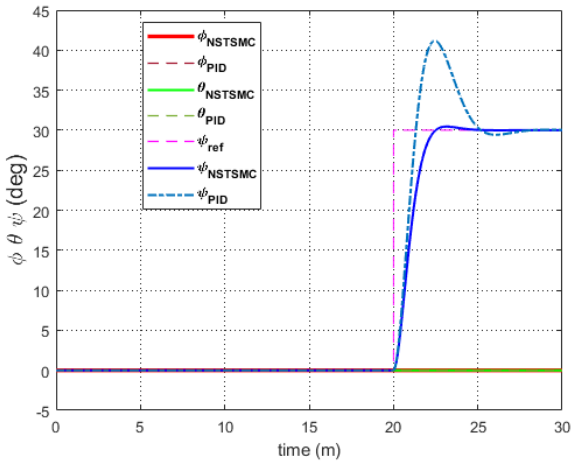

Figure 6. Roll (ϕ), Pitch (θ), Yaw (Ψ) angles

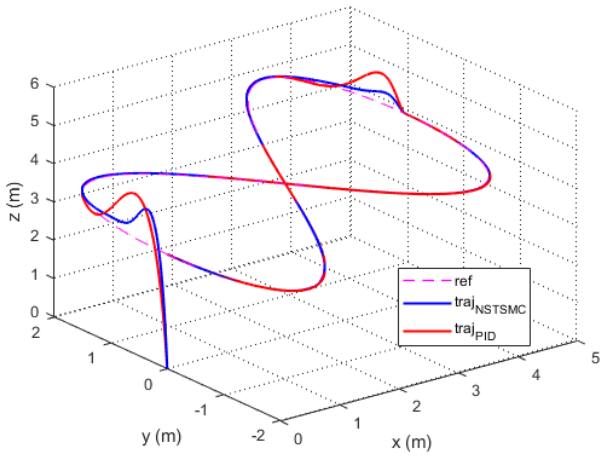

Figure 7. Hexacopter 3D trajectory under NSTSMC compared to PID

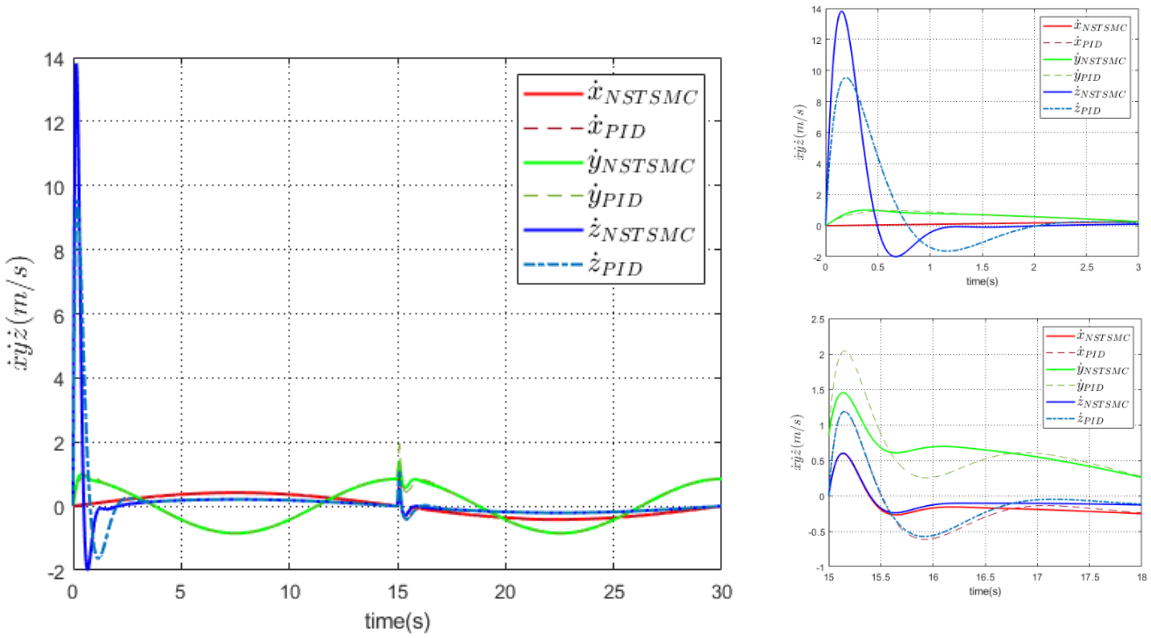

Figure 8. *X*, *Y*, *Z* velocities (with zoom)

Journal of Information Systems Engineering and Management
2025, 10(4)
e-ISSN: 2468-4376
https://www.jisem-journal.com/

Research Article

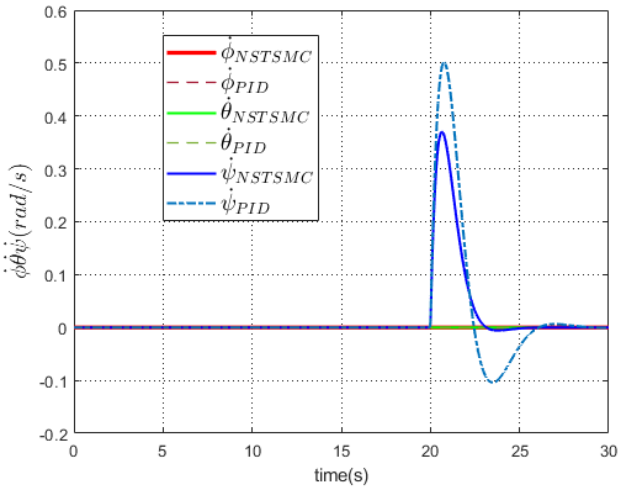

Figure 9. Roll *(ϕ)* , Pitch *(θ)* , Yaw *(Ψ)* velocities

The presented figures illustrate the performance of the Hexacopter following the trajectory. In Figs. 3 (a,b,c), and 4 the position and attitude can be analyzed. the desired flight path is followed by the Hexacopter, whose flight is slightly affected by the presence of *XYZ* disturbances (Fig.5). It can be observed that the trajectory tracking in the three directions is minimal in the NSTSMC case compared to the PID, especially in the *Z* direction where the hexacopter takeoff from the origin (0,0,0), the response was faster and the tracking error is less. The error is less noticeable in the x direction due to slow variation and the initial value of the X reference.

From *t = 20s* to *t = 30s*, the hexacopter changes its yaw angle (Fig. 4,) while moving to the point (0,0,4), the response of the PID is oscillatory which can affect the performance of the aircraft in a perturbed environment φ, and θ angles are regulated to 0 with negligible errors which indicate stability. According to Fig.6 and Fig.7. The NSTSMC control is done without excessive translational and angular speeds which enhance the life span of the UAV.

CONCLUSION

The objective of this work is to propose a control scheme for Hexacopter UAV trajectory tracking based on the sliding mode control. Initially, the non-linear mathematical model of the Hexacopter was derived using Newton-Euler's formulation. Then, a nonsingular fast terminal sliding mode controller is designed to make the system track the flight trajectory with a variation of the orientation angle. To test the robustness of the flight controller, perturbations were added to the experiment. The MATLAB-Simulink environment was used to evaluate the validity of the control and its performance compared to the classical PID controller. The results showed that the aircraft was able to reject perturbations that minimally affected the defined trajectory with no excessive effort in the case of the NSTSMC.

REFRENCES

[1] Sun, C., Agha, S. A., Mohamed, Z., & Shaheed, M. H. (2022). Optimised Sliding Mode Control of a Hexacopter: Simulation and Experiments. Electronics, 11(16), 2519

[2] Ye, J.; Wang, J.; Song, T.; Wu, Z.; Tang, P. (2021). Nonlinear Modeling the Quadcopter Considering the Aerodynamic Interaction. IEEE Access, 9, 134716–134732

[3] He, L., Tang, C. (2023). Two-Phase Non-Singular Terminal Sliding Mode Control of Nonlinear Systems. Applied Sciences, v.13, n. 23, p. 12684

[4] Claudio, R., Soria, C. M., Rossomando, F. G. (2019) . Identification and adaptive PID Control of a hexacopter UAV based on neural networks. Int. J. Adapt. Control Signal Process. v.33, n.1 , 74–91

[5] Erkol, H. O., (2018). Attitude controller optimization of four-rotor unmanned air vehicle," International Journal of Micro Air Vehicles, v.10, n.1, p.42–49

[6] Patel, K., Barve, J. (2014). Modeling, simulation and control study for the quad-copter UAV. In Proceedings of the 9th International Conference on Industrial and Information Systems (ICIIS), India, 15–17 December, p. 1–6
[7] Bolandi, H., Rezaei, M., Mohsenipour, R., Nemati, H., Smailzadeh, S. M. (2013). Attitude control of a quadrotor with optimized PID controller. Intelligent Control and Automation, v.4, n.3, p. 335–342
[8] Dong, W., Gu, G., Zhu, X., Ding, H. (2013). Modeling and Control of a Quadrotor UAV with Aerodynamic Concepts . World Academy of Science Engineering and Technology ,v.7, p377-385
[9] Yao, L., Cheng, M. (2019). Aerodynamic Performance of Hex-Rotor UAV Considering the Horizontal Airflow. Applied Sciences ,v.9, n. 22,p. 4797
[10] Rosales, C., Soria, C. M., Rossomando, F. G. (2019). Identification and adaptive PID Control of a hexacopter UAV based on neural networks. Internatinal Journal of Adaptive Control and Signal Processing, v. 33, p. 74-91
[11] Alaimo, A., Artale, V., Milazzo, C., Ricciardello, A., Trefiletti, L. (2013). Mathematical Modeling and Control of a Hexacopter. Proceedings of the International Conference on Unmanned Aircraft Systems (ICUAS), Atlanta, GA, USA, 28–31, p. 1043–105
[12] Song, H., Shaolin, H., Wenqiang, J., Qiliang, G. (2022). EKF-AF PID-Based Attitude Control Algorithm for UAVs . Hindawi Mobile Information Systems, v. 22.1
[13] Chiew, T.H., Lee, H.E., Lee, Y.K., Chang, K.M. (2021). Second Order Sliding Mode Controller for Altitude and Yaw Control of Quadcopter. Proceedings of the 11th IEEE International Conference on Control System, Computing and
[14] Engineering (ICCSCE), Penang, August, Malaysia 27–28, p. 97–102.
[15] Rosales, C., Soria, C. M., Rossomando, F. G. (2019). Identification and adaptive PID Control of a hexacopter UAV based on neural networks. International Journal of Adaptive Control and Signal Processing, v. 33, n. 1, p. 74–91
[16] Wang, T., Qin, R., Chen, Y., Snoussi, H. (2019). A reinforcement learning approach for UAV target searching and tracking," Multimedia Tools and Applications, v. 78, n. 4, p. 4347–4364
[17] Songming, J., Haiyue, G., Xiaokun, Z., Dengpan, L. (2020). Fault Tolerant Control Algorithm of Hexarotor UAV. Journal of Robotics , , Hindawi, v.20,n.16
[18] Chaoran, S., Agha, S. A., Zaharuddin, M., Shaheed, M. H. (2022). Optimised Sliding Mode Control of a Hexacopter: Simulation and Experiments. Electronics ,v.11, n.16, p. 2519
[19] Feng, Y., Xinghuo, Y., Han, F. (2013). On nonsingular terminal sliding-mode control of nonlinear systems. Automatica, v.49, n.6, p.1715-1722
[20] Ye, J., Wang, J., Song, T.,Wu, Z., Tang, P. (2021). Nonlinear Modeling the Quadcopter Considering the Aerodynamic Interaction. IEEE Access, 9, 134716–134732